

Influence of Decavanadate Clusters on the Rheological Properties of Gelatin

Florent Carn,[†] Madeleine Djabourov,^{*,‡} Thibaud Coradin,[†] Jacques Livage,[†] and Nathalie Steunou^{*,†}

UPMC Univ Paris 06, Collège de France, UMR-CNRS 7574, Laboratoire de Chimie de la Matière Condensée de Paris, F-75005, Paris, France, and Laboratoire de Physique Thermique, Ecole Supérieure de Physique et Chimie Industrielle, 75005 Paris, France

Received: March 12, 2008; Revised Manuscript Received: July 29, 2008

The influence of polyoxovanadate clusters ($[\text{H}_2\text{V}_{10}\text{O}_{28}]^{4-}$) on the thermo-reversible gelation of porcine skin gelatin solution (type A, $M_w \approx 40\,000\text{ g}\cdot\text{mol}^{-1}$, $\text{pH} = 3.4 \ll \text{isoelectric point (IEP)} \approx 8$) has been investigated as a function of temperature and vanadate concentration by combining rheology and microcalorimetry. This work shows that the rheological properties of the system depend on electrostatic interactions between $[\text{H}_2\text{V}_{10}\text{O}_{28}]^{4-}$ and positively charged gelatin chains. In a first stage, we describe the renaturation of the gelatin triple helices in the presence of decavanadate clusters. We reveal that, when gelatin chains are in coil conformation ($30\text{ }^\circ\text{C} < T < 50\text{ }^\circ\text{C}$), the inorganic clusters act as physical cross-linkers that govern the viscoelastic properties of the mixture with an exponential dependence of the (G' , G'') modulus with the vanadate concentration. Below $30\text{ }^\circ\text{C}$, we show that gelatin triple helix nucleation is slightly favored by the presence of vanadate, but above a helix concentration of $0.012\text{ g}\cdot\text{cm}^{-3}$, G' is fully governed by the helix concentration. During the melting process, we reveal the non-fully reversible behavior of the vanadate/gelatin rheological properties and the stabilization of gelatin triple helices due to vanadate species until $50\text{ }^\circ\text{C}$. This non-reversible character has also been observed in the same experimental conditions with collagen/vanadate solutions. This is the first time that such a stabilization of triple helices has been reported in the case of gelatin hydrogels chemically cross-linked or not. We propose to analyze these results by considering that triple helix aggregates should persist because of decavanadate bridging, that the nucleation of an extended triple helix network may induce a strong modification of the vanadate cross-linker distribution in the system, or both, thus promoting the formation of thermally stable vanadate/gelatin micro-gels in the dangling end of the triple helices.

I. Introduction

Natural macromolecules such as gelatin, alginate, cellulose, and so forth are an abundant source of raw materials that have attracted a great deal of interest due to their relatively low environmental and economical cost.¹ An actual promising perspective concerns the association between these biopolymers and functional additives such as polyoxometalate clusters (POMs)² via weak physical interactions. Such combinations can induce phase separation phenomenon that can be used in water treatment^{3a,b} or for protein purification.^{3a,c} In materials science, biological molecules have been recognized to exert a remarkable level of control over the mineral phase nucleation of biogenic inorganic materials, such as calcium carbonate and silica, and over the assembly of crystallites into complex structures required for biological function.⁴ This ability of biopolymers to direct the assembly of nanoscale building blocks into tailored structures in soft conditions is mainly based on their self-organization properties and the synergy observed between the inorganic and the organic components.⁴ It is expected that these bioinspired strategies can be extended to the integration of POMs into naturally occurring polymers in order to provide a convenient, low cost, and environmentally friendly way for processing functional bionanocomposites materials^{5,6} via soft chemical strategies.⁷

This assumption is strongly supported by the recent development of materials composed of biopolymers, such as charged polysaccharides or gelatin, and inorganic entities, such as clay minerals, double layered hydroxides, phosphates, and metal oxides, that show suitable properties notably for acting as active phases in electrochemical sensors.^{6–8}

It is therefore interesting to study the interactions in solution between POMs and biomacromolecules as it is the starting point for functional bionanocomposites processing into a number of forms such as monoliths, films, or even stable nanoparticle suspensions. In particular, it seems of primary importance to determine the phase behavior of the inorganic cluster/biopolymer mixture and the influence of small inorganic entities (diameter $\approx 1\text{ nm}$) displaying a high charge density on the very early stages of biomacromolecule conformation transition. Until very recently, to the best of our knowledge, no detailed studies were devoted to the biopolymer transition of conformation in the presence of multivalent polyoxometalate clusters with the size down to the limit of the colloidal domain.

In the present study, we report a detailed description of the porcine skin gelatin (type A, $M_w \approx 40\,000\text{ g}\cdot\text{mol}^{-1}$, $\text{pH} = 3.4 \ll \text{IEP} \approx 8$) transition of conformation in the presence of polyoxovanadate clusters by combining rheological and microcalorimetric investigations.

Gelatin is a polypeptide obtained by hydrolytic degradation of mammalian or fish collagen.⁹ This biopolymer is soluble in water at temperatures above the temperature of gelification (T_{gel} , which is close to $27\text{ }^\circ\text{C}$ for a mammalian gelatin) and forms reversible physical gels below T_{gel} .⁹ Here, T_{gel} is estimated as

* Corresponding author. E-mail: nathalie.steunou@upmc.fr (N.S.) and Madeleine.Djabourov@espci.fr (M.D.).

[†] Collège de France.

[‡] Ecole Supérieure de Physique et Chimie Industrielle.

the temperature for which the storage modulus (G') is equal to the loss modulus (G'') for a gelatin concentration of the order of 5 to 10%. This gel formation is due to the partial recovering of the triple-helix conformation of the native collagen.^{9,10b,c} For many applications in photographic, food, pharmaceutical, or cosmetics industry, addition of cross-linking agents leads to an enhancement of the mechanical and thermal properties of the protein gel over a large range of temperature and humidity level.^{9–14} Thus, in the past few years many investigations were carried out to better understand, experimentally and theoretically, the mechanisms and key-parameters governing the physical gelation of pure gelatin,¹⁰ gelatin in the presence of several chemical,¹¹ or physical cross-linkers such as copolymers,¹² polyelectrolytes,¹³ or anionic surfactants.¹⁴ The influence of multivalent counterions on biopolymer conformation has been extensively studied in the case of DNA¹⁵ and may be considered as a reference for similar studies on gelatin conformation which is still poorly documented so far.

The decavanadate ($[\text{H}_2\text{V}_{10}\text{O}_{28}]^{4-}$) entity is a small polyoxovanadate cluster (size ≈ 1 nm) that has received a great deal of attention in various domains ranging from materials science, where it is involved in the formation of multifunctional V_2O_5 ribbons,¹⁶ to biology, where its significant biological activity has motivated a great deal of research.^{3c,17}

We have established a phase diagram of the vanadate/gelatin mixture at $T = 40$ °C and pH 3.4.¹⁸ It clearly shows a two-step liquid–liquid phase separation process that is observed by increasing vanadate concentration. The characterization of colloidal solutions by liquid ^{51}V NMR spectroscopy and dynamic light scattering at different vanadate/gelatin ratio has given evidence that the decavanadate cluster and gelatin chains are the molecular species involved in this separation process. The experimental results are consistent with the formation of weakly charged colloidal aggregates due to electrostatic interactions between decavanadate anions and positively charged gelatin chains without perfect ion pairing. Upon increasing vanadate concentration, these aggregates rearrange in solution and condense into a microgel phase. This liquid–liquid separation process is fully consistent with a complex coacervation behavior mainly reported for organic biomacromolecules in the presence of proteins, surfactants, polyelectrolytes, or dendrimers.¹⁹ It is the first time that such a process is described for a biopolymer in interaction with polyoxometalate clusters. We have clearly shown that this separation process occurs typically at pH < 4.5. In this domain of pH and temperature, gelatin macromolecules are in a random coil conformation with fully protonated amine ($\text{p}K_a \text{ NH}_3^+/\text{NH}_2 \approx 10.5$) and carboxylic acid functions ($\text{p}K_a \text{ COOH}/\text{COO}^- \approx 4$) giving rise to a global positive charge (IEP ≈ 8). Thus, gelatin behaves like a weak cationic polyelectrolyte while the main vanadate species in solution at pH 3.4 are the anionic decavanadate clusters ($[\text{H}_2\text{V}_{10}\text{O}_{28}]^{4-}$, orange color) in equilibrium with cis-dioxocation (VO_2^+ , faintly yellow color).

The present study will be focused on the influence of vanadate species on the rheological properties of gelatin in the semidilute regime (typically [gelatin] = 10 wt % and $0 \leq [\text{vanadate}] \leq 72$ mM) at pH 3.4 and below the liquid–liquid phase separation threshold (homogeneous domain).

We describe respectively the influence of vanadate species on gelatin triple helices renaturation and melting in a temperature sweep between 50 and 20 °C by performing correlations between rheological and microcalorimetric experiments. All of the results are compared and discussed in the context of thermoreversible and chemically cross-linked gelatin gelation. The

melting of gelatin triple helices in presence of vanadate is also compared with that of soluble native collagen solutions in the same conditions. In the last part, a general mechanism that may explain our measurements is proposed.

II. Materials and Methods

Materials. All chemicals were commercially available and used without further purification.

Preparation of Vanadate Solutions. Polyoxovanadates have been prepared by two different methods. In the first one, the synthesis involves the acidification of an aqueous solution of sodium metavanadate NaVO_3 (Sigma, >99%, 0.5 M, pH = 8) according to a procedure currently used for the synthesis of vanadium oxide gels.¹⁶ Acidification of a $0.5 \text{ mol}\cdot\text{L}^{-1}$ metavanadate solution, with an initial pH close to 8, was performed using a proton exchange resin (DOWEX 50WX 4–100 mesh) at room temperature. A clear yellow solution (pH = 1) was obtained after full proton exchange that progressively turns into a red $\text{V}_2\text{O}_5\cdot n\text{H}_2\text{O}$ gel after about 12 h. For rheological investigations, the pH of the aqueous vanadate solution is adjusted to 3.4 with NaOH ($c = 2$ M) immediately after acidification. The temperature is rapidly raised to 50 °C. In the second route, aqueous solutions of sodium metavanadate NaVO_3 ($C = 0.2, 0.4, 0.6$, or 0.8 M depending on the desired final concentration) are directly acidified by an aqueous HCl solution (2 N). Since rheological and microcalorimetric measurements gave identical results for both procedures, samples were mainly prepared by the easiest second method.

Preparation of Gelatin Solutions. Commercial gelatin extracted from porcine skin (type A with a bloom of ~ 175 g corresponding to an average molecular weight of $\sim 40\,000$ g/mol and an IEP close to 8 according to the supplier) was purchased from Sigma-Aldrich. Gelatin solutions were prepared by swelling the gelatin granules in an aqueous solution during a minimum of 3 h at 5 °C. Gelatin was then dissolved at 50 °C using a magnetic stirrer for 30 min at 300 rpm. A viscosity of $9.9 \times 10^{-3} \text{ Pa}\cdot\text{s}$ has been measured for a 10 wt % pure gelatin solution at 45 °C.

Preparation of Gelatin/Vanadate Mixtures. When gelatin is dissolved, the pH is adjusted to 3.4 with an aqueous HCl solution (2 N) and the temperature is fixed at 50 °C. Then, 2 mL of the vanadate solution and 20 mL of the gelatin solution are mixed and stirred during 20 min at 300 rpm and 50 °C before performing the different characterizations. The as-prepared mixtures are homogeneous (below the phase separation threshold because of complex coacervation) in agreement with the vanadate/gelatin phase diagram recently established in the same experimental conditions.¹⁸ All samples are then rapidly carried over the rheometer or microcalorimeter with a vessel thermalized at 50 °C. The control of temperature, stirring rate, and time, during which the solution is kept at 50 °C, are critical parameters in the sample preparation since they may lead to a partial hydrolysis of gelatin thereby affecting the molecular weight distributions and consequently the rheological properties of gelatin solutions.^{9d} Moreover, the solutions that gelled did not completely recover their initial stage of dispersion after heating, because some local associations of the chains (especially by hydrophobic groups or entanglements) may persist. Higher temperatures or longer periods of heating that induce substantial degradation of gelatin must be avoided. Because of these constraints, each solution was used only once.

Preparation of Collagen/Vanadate Mixtures. Type I collagen helices were extracted from young rat tail tendon²⁰ and were stabilized at 20 °C in a solution of acetic acid (0.5 M).

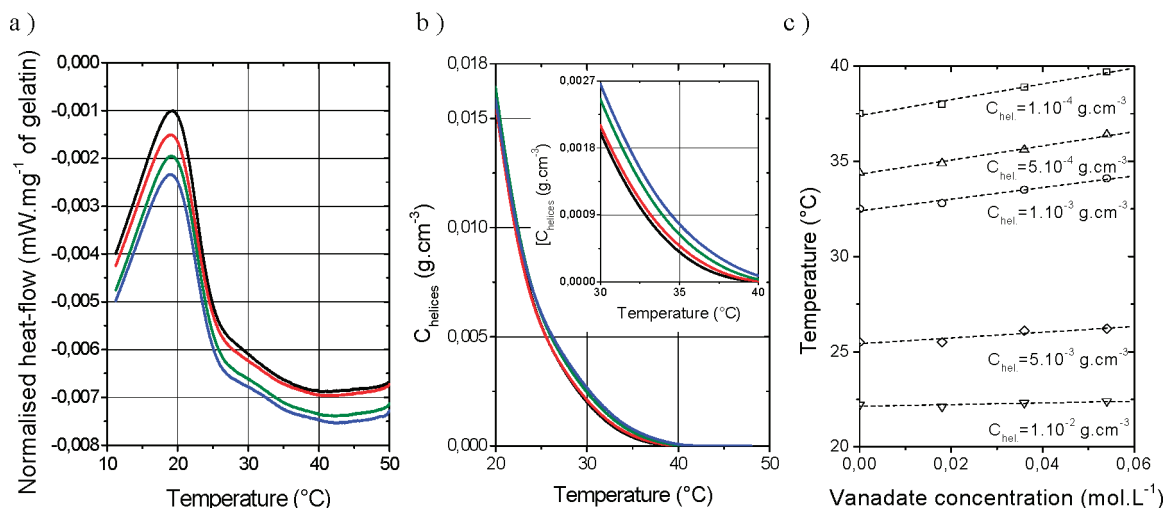


Figure 1. (a) Thermograms obtained by μ -DSC during the renaturation process ($v_{50\text{ }^{\circ}\text{C} \rightarrow 10\text{ }^{\circ}\text{C}} = 0.2\text{ }^{\circ}\text{C}\cdot\text{min}^{-1}$) for gelatin solutions ($[G] = 10\text{ wt } \%$, $\text{pH} = 3.4$) displaying different vanadate concentrations: $[V] = 0\text{ M}$ (black curve), $[V] = 18\text{ mM}$ (red curve), $[V] = 36\text{ mM}$ (green curve), $[V] = 54\text{ mM}$ (blue curve); (b) Helices concentration (determined from Figure 1a) as a function of temperature; (c) Temperature at which a given C_{hel} is obtained as a function of vanadate concentration. The dashed lines correspond to linear fits of experimental data.

Collagen/vanadate mixtures were prepared at $5\text{ }^{\circ}\text{C}$ by adding 90 mg of aqueous vanadate solution of different concentrations in 650 mg of an aqueous collagen solution ($[\text{collagen}] = 3.5\text{ mg}\cdot\text{mL}^{-1}$). The pH of each solution was previously adjusted to 2.3 with acetic acid, and the concentration of the vanadate precursor solutions was chosen in order to reach the following concentrations: $[V] = 0, 0.003, 0.006,$ and 0.032 M after addition. For all of the vanadate/collagen solutions, the Na^{+} concentration is equal to the vanadate concentration since the source of Na^{+} cations is the vanadate precursor NaVO_3 . The samples prepared with $[V] = 0.006\text{ M}$ are heterogeneous since they consist of a yellow gel in the upper part and a liquid in the lower part. Stirring the samples for 2 h at $20\text{ }^{\circ}\text{C}$ leads to biphasic heterogeneous samples. Therefore, we have decided to perform measurements on samples prepared without stirring at $20\text{ }^{\circ}\text{C}$ in order to avoid any denaturation of the native collagen before performing μ -DSC measurements.

Rheology. Rheology measurements were performed with a controlled strain rheometer AR G2 from TA Instruments using a magnetic thrust bearing technology and operating in the oscillatory mode with a cone and plate geometry (diameter, 60 mm; gap, 54 μm ; angle, 2°). A lid with a solvent trap was used to minimize evaporation. Light silicone oil was also poured on the top of the solvent trap, and the border of the lid was greased to limit evaporation. The temperature was controlled by a Peltier device with an accuracy of $0.1\text{ }^{\circ}\text{C}$. Cooling and heating ramps of $0.2\text{ }^{\circ}\text{C}\cdot\text{min}^{-1}$ were applied between 50 and $20\text{ }^{\circ}\text{C}$ with a gap compensation of $0.5\text{ }\mu\text{m}$ in this range of temperature. The rheometer worked with a controlled strain of 1% in order to be in the viscoelastic linear regime in the course of gelation. Most of the rheological experiments presented in this study were performed at a single frequency of 1 Hz, but additional measurements were also performed at 0.1 and 10 Hz (Figure 3, Supporting Information). At $f = 1\text{ Hz}$, the linear response regime was measured for strains up to 5% for the lower vanadate concentration ($c = 0.018\text{ M}$) and up to 1% for the higher vanadate concentration ($c = 0.072\text{ M}$).

Microcalorimetry (μ DSC). Microcalorimetry has been used to follow the gelatin conformational transition in presence of vanadate species. Our instrument was a micro-DSC III from Setaram using closed vessels ($V_{\text{batch}} = 850\text{ }\mu\text{L}$) and allowing a resolution of $0.03\text{ }\mu\text{W}$. Cooling and heating ramps were applied

between 50 and $10\text{ }^{\circ}\text{C}$ with a scanning rate of $0.2\text{ }^{\circ}\text{C}\cdot\text{min}^{-1}$. At $10\text{ }^{\circ}\text{C}$, an isotherm of 1 h was applied between the cooling and the heating ramps. Some experiments were performed with scanning rates down to $0.05\text{ }^{\circ}\text{C}\cdot\text{min}^{-1}$ in order to check the kinetic dependence of the result (Figure 2, Supporting Information).

Optical Rotation. In the case of transparent pure gelatin solutions, the triple helix concentration has also been monitored by optical rotation. The experiments were carried out as previously described by Joly-Duhamel et al.^{10b,c}

Determination of Helix Concentration. By following the methodology introduced by Hellio-Serughetti et al.,^{11c,d} the optical rotation and the total heat released (calculated from the heat flux by integration, after correction for the baseline) of pure gelatin solution ($c = 10\text{ wt } \%$, $\text{pH} = 3.4$) were measured versus time and temperature (Figure 1, Supporting Information). From these experiments, it is possible to extract the enthalpy of coil/helix transition per residue, which is for our gelatin sample: $\Delta H_{\text{Coil} \leftrightarrow \text{Hel}} = 5.5 \pm 0.2\text{ kJ}\cdot\text{mole}^{-1}$ per residue. This value is in agreement with the results given by Joly-Duhamel et al.^{10b} or more recently El Harfaoui et al.^{10f} and is also close to the enthalpy of native collagen triple helix melting.²¹

The μ -DSC measurements on vanadate/gelatin solutions performed during the cooling process reveal the absence of endothermic peak between 50 and $40\text{ }^{\circ}\text{C}$ (Figure 2 Supporting Information). Therefore, we ascribe the whole heat-flow peak to the gelatin triple helix transition of conformation. Assuming that the enthalpy of transition of gelatin conformation is generally recognized to be unmodified during chemical cross-linking,^{11c,d} we can make the hypothesis that $\Delta H_{\text{Coil} \leftrightarrow \text{Hel}} = 5.5\text{ kJ}\cdot\text{mole}^{-1}$ whatever the vanadate concentration. The triple helix concentration in decavanadate–gelatin solutions has been determined by μ -DSC since the yellow color of these solutions prevents optical rotation measurements.

III. Results and Discussion

(a) Gelatin Triple-Helices Renaturation in Presence of Vanadate. Figure 1a represents thermograms obtained for gelatin solutions containing different vanadate concentrations ranging from 0 M to 0.054 M before baseline correction.

In the case of pure gelatin solution (black curve in Figure 1a), the triple helix renaturation is characterized by a broad

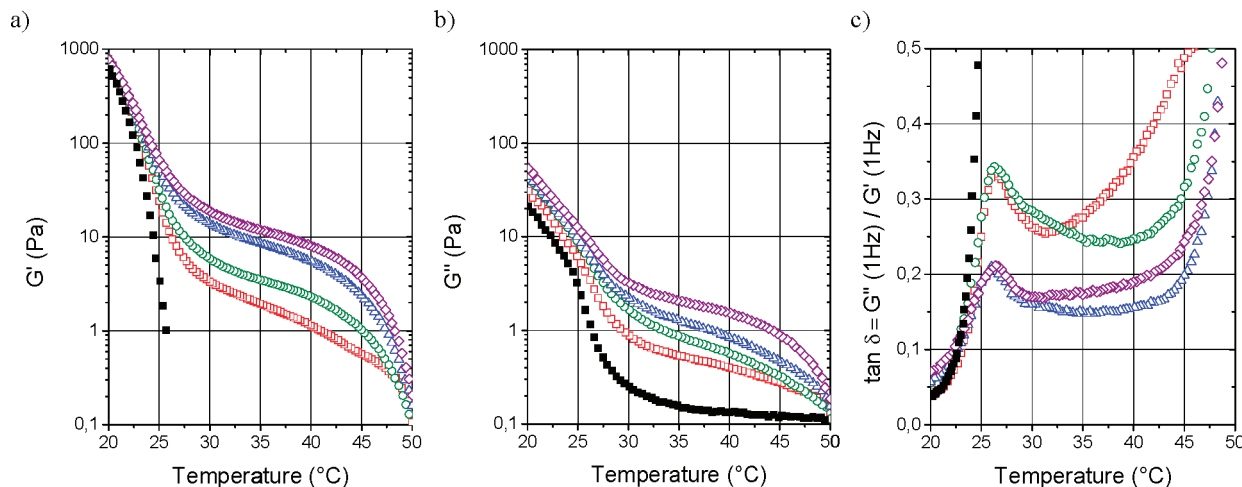


Figure 2. Evolution of the storage G' (a) and loss G'' (b) modulus as a function of temperature during the cooling ramp ($v_{50\text{ }^{\circ}\text{C}-20\text{ }^{\circ}\text{C}} = 0.2\text{ }^{\circ}\text{C}\cdot\text{min}^{-1}$) for gelatin solutions ($[G] = 10\text{ wt } \%$, $\text{pH} = 3.4$) displaying different vanadate concentrations: 0 M (■), 0.018 M (□, red), 0.036 M (○, green), 0.054 M (Δ, blue) and 0.072 M (◇, purple). (c) $\tan \delta = G''/G'$; as a function of temperature for the same previous samples.

exothermic signal displaying a maximum for $T = 19.0\text{ }^{\circ}\text{C}$. In the presence of vanadate species, the curves display almost the same shape with a single maximum around $T = 19.0\text{ }^{\circ}\text{C}$. After baseline correction and integration of the heat flow signal as a function of time, we have derived the helix concentration as a function of temperature (see Experimental Section) for the different samples (Figure 1b). In the absence of vanadate, the triple helices start to form ($C_{\text{hel.}} = 1.10^{-4}\text{ g}\cdot\text{cm}^{-3}$) around $37.5\text{ }^{\circ}\text{C}$, while in the presence of vanadate, the renaturation seems to start at slightly higher temperatures ($T = 39.7\text{ }^{\circ}\text{C}$ for $C_{\text{hel.}} = 1.10^{-4}\text{ g}\cdot\text{cm}^{-3}$ and $[V] = 0.054\text{ M}$). The influence of vanadate on triple helix formation can be observed between $T = 23\text{ }^{\circ}\text{C}$ and $T = 40\text{ }^{\circ}\text{C}$ but is negligible at lower temperatures. Figure 1c represents in a more explicit manner the almost linear relation existing between the vanadate concentration and the temperature for which a given concentration of triple helix is present in the system.

In summary, unlike chemically cross-linked gelatin,^{11c,d} the helix renaturation is not deeply affected by the presence of vanadate species since a $C_{\text{hel.}} = 0.016\text{ g}\cdot\text{cm}^{-3}$ is obtained at $20\text{ }^{\circ}\text{C}$ whatever the vanadate concentration. However, decavanadate species favor the nucleation of gelatin triple helix at temperatures between 23 and $40\text{ }^{\circ}\text{C}$. These results corroborate observations performed by Gillmor et al. on sodium poly(styrenesulfonate)/gelatin mixtures.^{13b}

In parallel, rheological investigations were performed on the same samples using the same thermal protocol, and the results were correlated to that of microcalorimetry. Figure 2a,b shows respectively the evolution of the storage (G') and loss (G'') moduli as a function of temperature for an aqueous gelatin solution ($[G] = 10\text{ wt } \%$, $\text{pH} = 3.4$) with different vanadate concentrations.

In the absence of vanadate, the pure gelatin solution behaves like a newtonian liquid ($G' \approx 0\text{ Pa}$) between $50\text{ }^{\circ}\text{C}$ and $27\text{ }^{\circ}\text{C}$. Below $27\text{ }^{\circ}\text{C}$, a measurable storage modulus appears and increases rapidly until overcoming the viscous modulus at $24.6\text{ }^{\circ}\text{C}$. According to the gelatin master curve of elasticity introduced by Joly-Duhamel et al.,^{10b,c} the evolution of the G' modulus arises from the formation of an extended triple-helix network. Below a critical triple-helix concentration ($C_{\text{hel.}}^* \approx 0.0035\text{ g}\cdot\text{cm}^{-3}$), there is no macroscopic network. In contrast, immediately above $C_{\text{hel.}}^*$, a sol–gel transition which is analogous to a percolation transition occurs, and a steep increase of the storage modulus is observed. A physical gel of gelatin with

elastic properties is then formed. This physical gel can be described as an entangled network of rigid triple helices that are connected via flexible links.

In the presence of vanadate species, a significant G' modulus can be measured from the starting point of the cooling ramp at $50\text{ }^{\circ}\text{C}$ down to $27\text{ }^{\circ}\text{C}$ where pure gelatin solution has no elastic modulus. According to μ -DSC (Figure 1), only a few triple helices are formed in this range of temperature ($C_{\text{hel.}} < C_{\text{hel.}}^*$). Therefore, we can reasonably explain these rheological measurements by electrostatic cross-linking action of decavanadate anions with protonated amine functions of the gelatin chains. Obviously, in absence of a triple helix network, between $50\text{ }^{\circ}\text{C}$ and $27\text{ }^{\circ}\text{C}$, the elastic contribution is directly related to the cross-linking density and thus to the vanadate concentration. Below $27\text{ }^{\circ}\text{C}$, all of the G' curves raise up in the same manner as pure gelatin solutions. The contribution of vanadate to G' is negligible at $20\text{ }^{\circ}\text{C}$ where the modulus is dominated by the triple helices. According to Figure 2a, G' at $30\text{ }^{\circ}\text{C}$ varies between 3.3 Pa and 18.6 Pa depending on vanadate concentration ($0 \leq [V] \leq 0.054\text{ M}$), while $G' = 770\text{ Pa}$ at $20\text{ }^{\circ}\text{C}$ independently of vanadate concentration.

As shown in Figure 2b, the viscous component (G'') is also strongly affected by the presence of vanadate species. It is important to note that, in the presence of vanadates, $G' \geq G''$ over the whole range of temperature. For temperatures above $27\text{ }^{\circ}\text{C}$, G'' increases with the vanadate concentration. Below $27\text{ }^{\circ}\text{C}$, in contrast to the storage modulus behavior, G'' still exhibits a weak but observable dependence on the vanadate concentration in presence of the triple helix network. Below $27\text{ }^{\circ}\text{C}$, decavanadate clusters may interact with dangling chains and loops that contribute to the dissipation of energy, while the triple-helix network seems to govern elasticity.

To conclude on the rheological investigations, we considered the loss angle evolution ($\tan \delta = G''/G'$) represented in Figure 2c. In a pure gelatin solution, $\tan \delta$ decreases from ∞ to 0 because the G' modulus tends to zero for temperatures above $30\text{ }^{\circ}\text{C}$. In the presence of vanadates, $\tan \delta$ can be measured along the entire temperature range, and the curves display a different shape. In a first stage, for $35\text{ }^{\circ}\text{C} < T < 50\text{ }^{\circ}\text{C}$, $\tan \delta$ decreases in parallel with the formation of an elastic network by decavanadate cross-links. For temperatures between $35\text{ }^{\circ}\text{C}$ and $27\text{ }^{\circ}\text{C}$, $\tan \delta$ curves increase while both G' and G'' also increase. In a last stage, for temperatures below $27\text{ }^{\circ}\text{C}$, all of the $\tan \delta$ curves decrease again like a pure gelatin sample. An

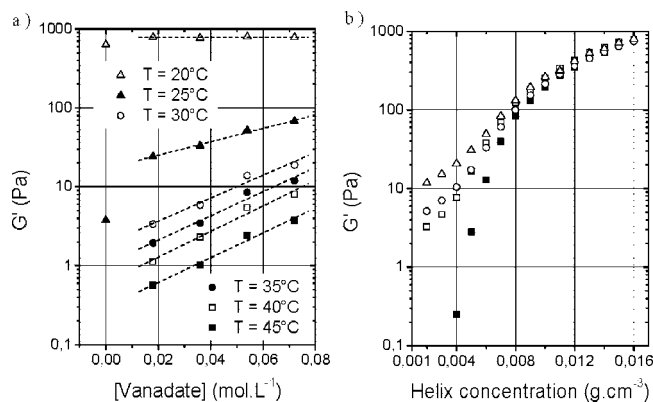


Figure 3. (a) Storage modulus (G') as a function of vanadate concentration for different temperatures (during the cooling ramp). The dashed lines correspond to exponential fits of experimental data concerning samples containing vanadate species. (b) Storage modulus as a function of helix concentration for gelatin solutions ($[G] = 10$ wt %, pH = 3.4) with different vanadate concentrations: 0 M (■), 0.018 M (□), 0.036 M (○), 0.054 M (Δ).

accurate observation of the different G' and G'' curves indicates that the helix network formation induces an increase in both G' and G'' values but not exactly for the same temperature. In fact, G'' starts to increase at a slightly higher temperature ($T \approx 30^\circ\text{C}$, $\tan \delta$ increases), then G' increases ($T \approx 27^\circ\text{C}$, $\tan \delta$ decreases), and as a consequence this gap of temperature is responsible for the emergence of a peak at 27°C . The reason why G'' increases at higher temperatures than G' can be understood by taking into account that triple-helices start to form between 39°C and 37.5°C depending on vanadate concentration, while G' starts to be measurable from 27°C for the pure gelatin solution. Therefore, according to the percolation model proposed by Joly-Duhamel et al.,^{10b,c} the first triple helices formed below C_{hel}^* or for $27^\circ\text{C} \leq T \leq 37^\circ\text{C}$ should be isolated or form mesoscopic clusters. The formation of independent triple helices should promote the formation of dangling ends or loops which contribute to dissipation of energy (increase of G'' modulus) and not to the elastic modulus.

It is worth noticing that G' , G'' , and the loss angle display the same global behavior in a large range of frequency between 0.1 and 10 Hz (see Figure 3 Supporting Information) even if a significant dependence of frequency exists above 25°C .

In summary, the loss angle plots provide a clear picture of the formation of the different physical networks. In fact, one can distinguish three main domains of network connectivity: (i) for $35^\circ\text{C} \leq T \leq 50^\circ\text{C}$, decavanadates cross-link the gelatin coils into a weak physical network ($\tan \delta$ decreases); (ii) for $27^\circ\text{C} \leq T \leq 35^\circ\text{C}$, triple helices nucleate in the vanadate/gelatin network ($\tan \delta$ increases); (iii) for $20^\circ\text{C} \leq T \leq 27^\circ\text{C}$, an extensive triple-helix network of gelatin chains grows and develops rapidly to fully govern the elastic properties of the system ($\tan \delta$ decreases).

In a last stage, in order to clearly show how the two types of physical bonds contribute to the network elasticity, the evolution of G' was plotted respectively as a function of helix concentration and vanadate concentrations (Figure 3a,b). Figure 3a represents the relation between G' and vanadate concentrations for different temperatures. For $T \geq 30^\circ\text{C}$, the exponential dependence of the storage modulus on the vanadate concentration is evidenced ($G' \propto e^{S'[\text{vanadate}]}$ with $S' = 15.4 \pm 0.5 \text{ M}^{-1}$ for $30^\circ\text{C} \leq T \leq 45^\circ\text{C}$, see Figure 3a). In the same way, the loss moduli depicts an exponential dependence with vanadate concentration ($G'' \propto e^{S''[\text{vanadate}]}$ with $S'' = 10.2 \pm 0.5 \text{ M}^{-1}$ for

$30^\circ\text{C} \leq T \leq 45^\circ\text{C}$, see Figure 4a Supporting Information). Below this temperature, the influence of vanadate decreases until 20°C where the influence of vanadate has almost completely disappeared. It is worthwhile noticing that the relation between G' and vanadate concentration could alternatively be fitted by a power law (Figure 5 Supporting Information). By taking into account the limited range of vanadate concentration currently studied, an exponential representation is preferred. Figure 3b represents the relation between G' and the helix concentration calculated from Figure 1b. When considering pure gelatin, one can observe that, above a helix concentration threshold (C_{hel}^*) of about 0.004 g cm^{-3} , the G' modulus increases rapidly. This evolution was observed on the master curve of gelatin elasticity by using optical rotation measurements.^{10b,c} When vanadate species are present in the system, a physical gel is already formed at low helix concentration ($C_{hel} < C_{hel}^*$) and a G' value independent of helix concentration is observed and increase with vanadate concentration. For higher helix concentrations, all of the G' values increase smoothly and converge towards the master curve. The presence of vanadate cross-links delayed slightly the G' convergence toward the master curve, but for $C_{hel} \geq 3C_{hel}^* = 0.012 \text{ g cm}^{-3}$, the vanadate contribution to elasticity becomes negligible. It is worth noticing that in the presence of an extended triple helix network the loss modulus keeps a strong dependence on the vanadate concentration ($G'' \propto e^{S''[\text{vanadate}]}$ with $S'' = 5.0 \pm 0.8$ for $20^\circ\text{C} \leq T \leq 25^\circ\text{C}$, see Figure 4a Supporting Information) in contrast with results obtained with chemically cross-linked gelatin.^{10b,c}

(b) Gelatin Triple-Helices Melting in Presence of Vanadates. In this section, we study the effect of vanadates on the triple helix melting by considering the behavior of the same previous samples during the heating ramp (see experimental section).

Figure 4a,b represents respectively the evolution of G' and G'' during the whole thermal treatment (cooling and heating successively) for a pure aqueous gelatin solution ($[G] = 10$ wt %, pH = 3.4) and a gelatin solution containing vanadates ($[V] = 0.072 \text{ M}$).

In the absence of vanadate, the gelatin solution recovers its initial Newtonian character ($G' \approx 0 \text{ Pa}$, $G''_{cooling} \approx G''_{heating}$) above 31°C due to triple helix melting in fair agreement with a fully thermo-reversible gelation process. In the presence of vanadate, one can observe a partial reversibility of the gelation process. In fact, the evolution of G' and G'' curves between 20 and 25°C are quite similar to those of gelatin, but then these curves tend to decrease much slower by increasing temperature. Above 40°C , G' moduli finally reach a constant value while G'' moduli are subject to a small decline. At 50°C , the storage modulus is significantly higher than the loss modulus suggesting that a vanadate–gelatin network is preserved upon heating above 30°C .

Figure 5 shows that these striking results are clearly related to the vanadate concentration. The discrepancy observed between the G' and the G'' behaviors in this second part of the heating ramp results into a distinct $\tan \delta$ peak (Figure 5c) centered around 32°C which is followed by a monotonous decrease until 50°C in contrast to the renaturation process (Figure 2c).

Furthermore, similar rheological behaviors have been observed in a large range of frequency between 0.1 and 10 Hz (see Figure 3 Supporting Information).

Figure 6 represents the influence of the vanadate concentration on the storage modulus during the heating ramp and should be compared to Figure 3a. The storage modulus (G') is almost

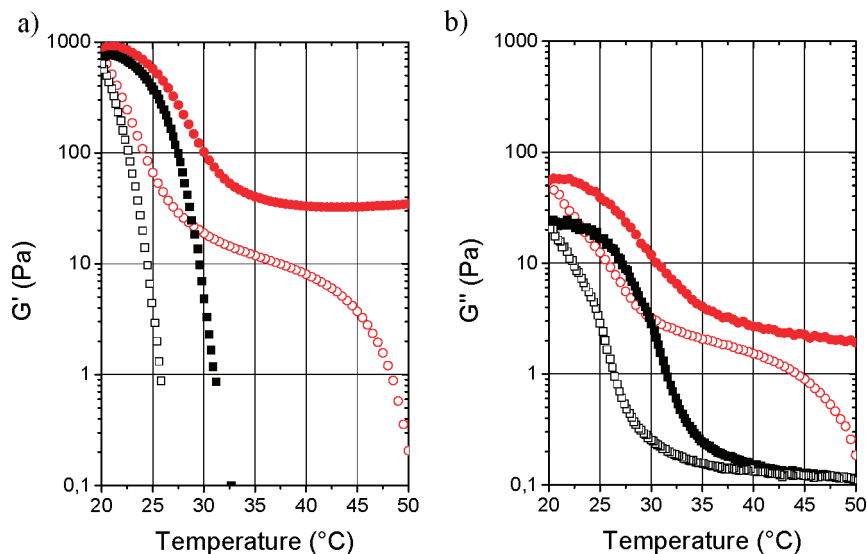


Figure 4. Evolution of the storage G' (a) and loss G'' (b) moduli as a function of temperature during the cooling (opened symbols) and the heating (filled symbols) ramps at $v_{50\text{ }^{\circ}\text{C} \rightarrow 20\text{ }^{\circ}\text{C}} = 0.2\text{ }^{\circ}\text{C} \cdot \text{min}^{-1}$, for pure gelatin solutions ($[G] = 10\text{ wt } \%$, black squares) and gelatin solution ($[G] = 10\text{ wt } \%$) containing 0.072 M of vanadate species (red circles).

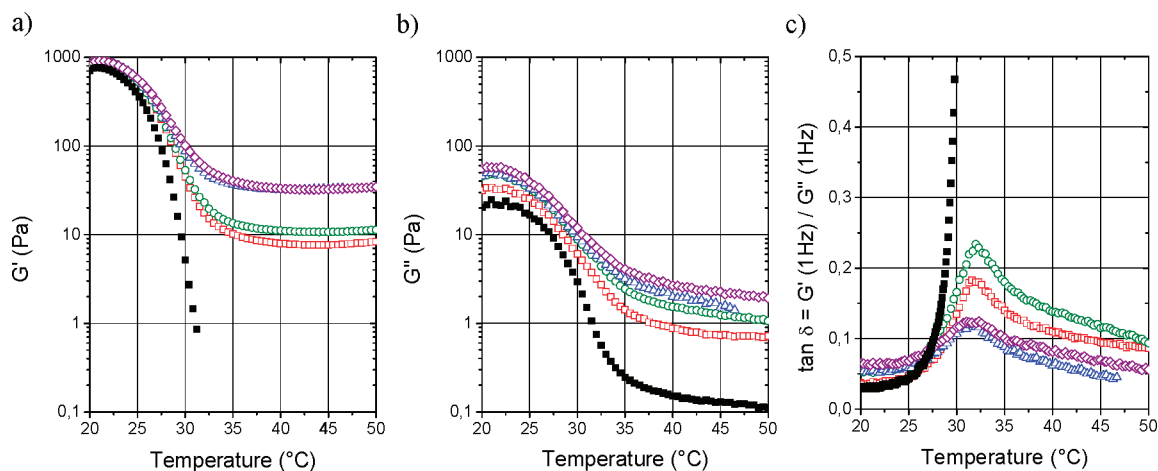


Figure 5. Evolution of the storage (a) and loss (b) moduli as a function of temperature during the melting ramp for gelatin solutions ($[G] = 10\text{ wt } \%$, pH = 3.4) displaying different vanadate concentrations: 0 M (■), 0.018 M (□, red), 0.036 M (○, green), 0.054 M (Δ, blue) and 0.072 M (◇, purple). (c) $\tan \delta = G''/G'$ as a function of temperature for the same previous samples.

independent on vanadate concentration below 25 °C and starts to increase with vanadate concentration at 30 °C. Above 35 °C, the different curves exhibit almost the same exponential law between G' and vanadate concentration ($G' \propto e^{S'[\text{vanadate}]}$) with $S' = 12.7 \pm 0.5$ for $35\text{ }^{\circ}\text{C} \leq T \leq 45\text{ }^{\circ}\text{C}$, see Figure 6). In contrast to the renaturation process, this relation is weakly affected by temperature and presents a slope notably smaller than the one measured during the renaturation process: $S_{\text{melting}} = 12.7 \pm 0.5\text{ M}^{-1} < S_{\text{renaturation}} = 15.4 \pm 0.5\text{ M}^{-1}$ for $35\text{ }^{\circ}\text{C} \leq T \leq 45\text{ }^{\circ}\text{C}$. These two points may suggest the formation of a more stable vanadate/gelatin network and a modification of the vanadate cross-links distribution in the system.

Micro-DSC measurements were also performed during the heating ramp (see details in Experimental Section) in order to estimate the reversibility of the transition of gelatin conformation. Figure 7a represents the broad endothermic signals obtained by μ -DSC during the triple helices melting. As observed during the renaturation process, the presence of vanadate does not strongly affect the thermogram shape. The triple-helix concentrations have been deduced by integration of the different signals after baseline correction and are represented as a function of temperature in Figure 7b. First of all, one can observe that, in

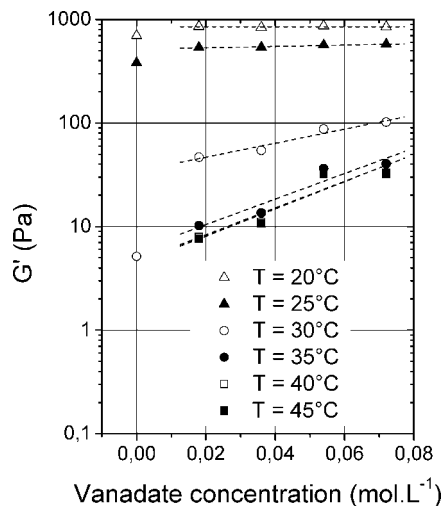


Figure 6. Storage modulus (G') as a function of vanadate concentration for different temperatures (during the heating ramp). The dashed lines correspond to exponential fits of experimental data concerning samples containing vanadate species.

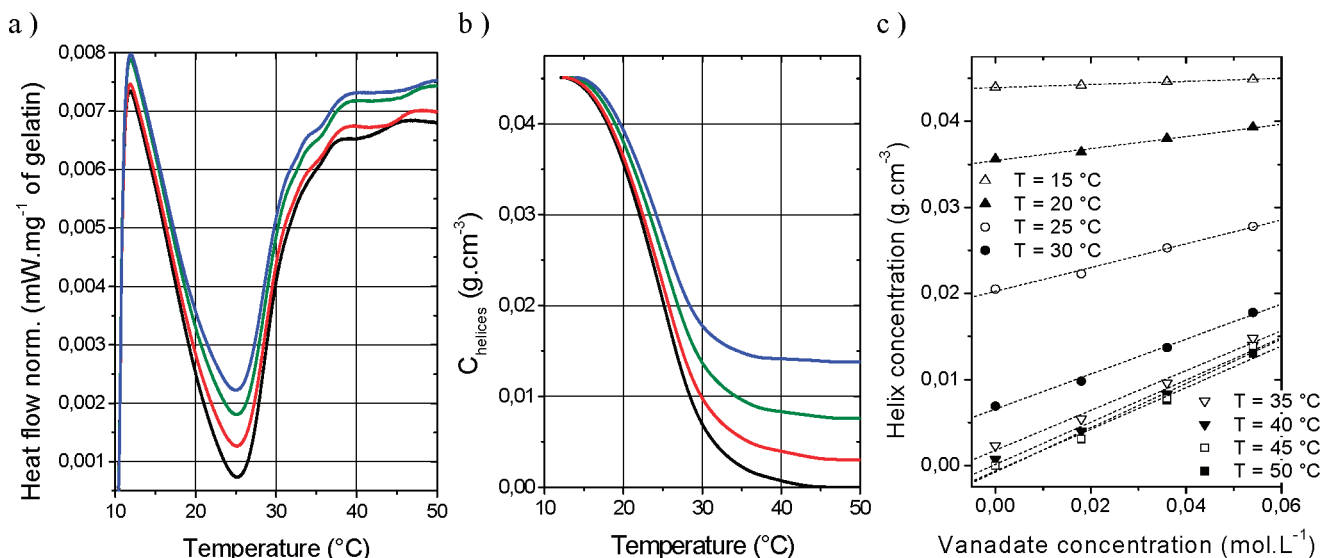


Figure 7. (a) Thermograms obtained by μ -DSC during the melting process ($v_{10}^{\circ\text{C} \rightarrow 50^{\circ\text{C}}} = 0.2^{\circ}\text{C} \cdot \text{min}^{-1}$) of gelatin solutions ([G] = 10 wt %) displaying different vanadate concentrations: [V] = 0 mM (black curve), [V] = 0.018 M (red curve), [V] = 0.036 M (green curve), [V] = 0.054 M (blue curve). (b) C_{hel} as a function of temperature for the same previous samples. (c) C_{hel} as a function of vanadate concentration for the same previous samples at different temperatures. The dashed lines correspond to linear fits of experimental data.

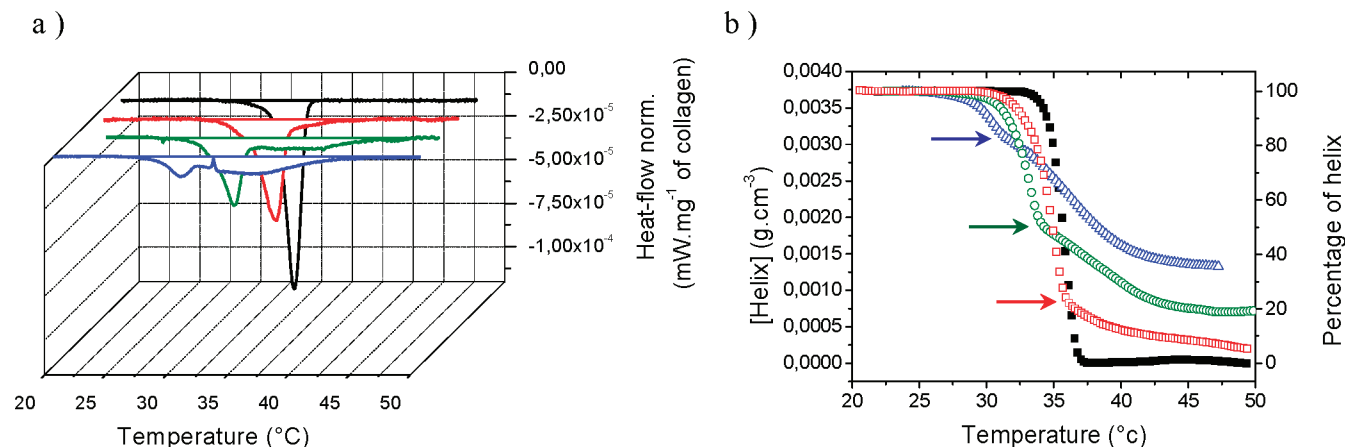


Figure 8. (a) Thermograms obtained by μ -DSC during the melting process ($v = 0.2^{\circ}\text{C} \cdot \text{min}^{-1}$) of native collagen solutions ([Collagen] = 0.3 wt %) with different vanadate concentrations: [V] = 0 M (black curve), [V] = 0.003 M (red curve), [V] = 0.006 M (green curve), [V] = 0.032 M (blue curve). (b) Helix concentration as a function of temperature for the same previous samples. The colored arrows indicate the helix concentration for which a variation of the slope is observed on the corresponding [helix] = $f(T)$ curves (each arrow is associated to the curve of the same color).

the presence of vanadates, the triple helix melting is not fully reversible. For the same initial triple helix concentration ($C_{\text{hel}} = 0.045 \text{ g} \cdot \text{cm}^{-3}$ at 15 $^{\circ}\text{C}$), the amount of melted helices at 50 $^{\circ}\text{C}$ decreases in the presence of vanadates. It is important to note that the same behavior has also been observed even by using a very low rate of temperature sweep ($v = 0.05^{\circ}\text{C} \cdot \text{min}^{-1}$, Figure 2 Supporting Information) suggesting that this result is not incidentally due to the heating rate. The representation of the helix concentration as a function of vanadate concentration (Figure 7c) reveals that the amount of residual triple helices is dependent on vanadate concentration and temperature from 20 to 30 $^{\circ}\text{C}$ and is only dependent on vanadate concentration above 35 $^{\circ}\text{C}$ following a unique linear law.

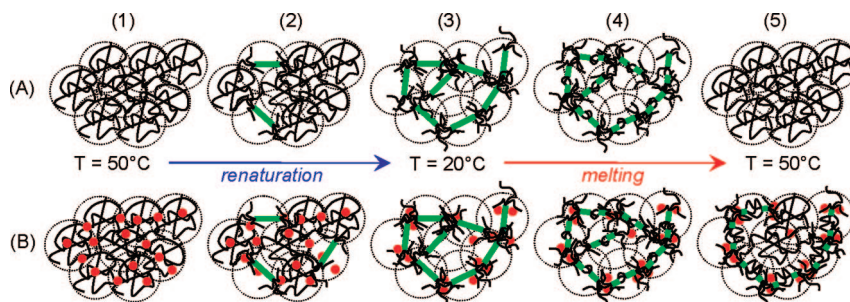
To the best of our knowledge, this is the first time that such triple helix stabilization until 50 $^{\circ}\text{C}$ is reported in the case of gelatin hydrogels chemically cross-linked or not. In order to ascertain this unexpected effect of vanadate and to estimate the specific influence of these inorganic species toward the triple helix thermal denaturation, we have studied native collagen/vanadate mixtures by μ -DSC.

(c) Native Collagen Denaturation in Presence of Vanadate.

We have performed μ -DSC measurements on native collagen (fully composed of triple helices) solutions containing different vanadate concentrations ranging from 3 mM to 32 mM. It is important to notice that vanadate addition at 5 $^{\circ}\text{C}$ induces the gelification of the upper part of the samples at intermediate vanadate concentration ([V] = 6 mM) and a macroscopic phase separation for the more concentrated sample ([V] = 32 mM) giving rise to an orange viscous lower phase similar to the coacervate phase obtained in the case of gelatin/decavanadate mixtures.¹⁸ Therefore, in contrast to gelatin, μ -DSC measurements presented here were performed on heterogeneous samples for [V] = 6 mM and 32 mM. Nevertheless, this study enables some qualitative observations that ascertain the results obtained on gelatin.

As expected, the denaturation of the pure native collagen solution is characterized by a sharp endothermic peak centered at 35 $^{\circ}\text{C}$ (black curve in Figure 8a). In these conditions, the evolution of the helix concentration as a function of temperature can be determined (black curve in Figure 8b) without ambiguity.

SCHEME 1: Proposed Schematic Representation of the Gelatin Triple Helix Renaturation (from (1) to (3)) and Melting (from (3) to (5)) for a Pure Gelatin Solution in the Semi-Dilute Regim (A) and for a Gelatin/Vanadate Mixture at the Same Gelatin Concentration (B)^a



^a The red disks represent decavanadate species; the green rods represent triple helices; the black solid lines represent gelatin chains, and the dotted circles represent the initial size of the gelatin chains in coil conformation at 50 °C.

One can observe that all the triple helices are melted in a very narrow range of temperatures between 33 and 37 °C.

In the presence of vanadates, the endothermic signal is characterized by a drastic broadening and a strong decrease of the heat exchanged during the melting process (Figure 8a). For the more concentrated solutions ($[V] = 6$ mM and $[V] = 32$ mM in Figure 8a), the endothermic peak seems to gradually develop a bimodal character. Considering the helix concentration evolution with temperature (Figure 8b), one can observe that the shape of the curves evolves from a steep transition to a very progressive one and that the total amount of melted triple helices is significantly lowered in the presence of vanadates. Moreover, the temperature for which the collagen denaturation starts is notably reduced by increasing vanadate concentration with a factor of about $0.2\text{ °C} \cdot \text{mM}^{-1}$ of vanadate. Taking into account the shape of the different curves, one can observe that, in contrast to the pure collagen solution, the triple helix melting observed in the presence of vanadates follows a two-step process. In a first stage, a fraction of helices is melted with a steep slope versus temperature in the same manner as pure collagen, and then a second fraction of helices is melted with a very progressive thermal transition (the transition between these two stages is evidenced by colored arrows in Figure 8b). The helix concentration for which the transition occurs increases with vanadate concentration suggesting that the inorganic clusters stabilize the second population of triple helices.

The picture that emerges from these μ -DSC measurements is that the vanadate species seem to have an ambivalent influence on collagen triple helix stability. However, these results can be understood by taking into account the inhomogeneous character of the different samples and the influence of electrostatic interactions on the collagen conformation.^{22,23} In fact, several studies have already reported the subtle influence of ionic species on the collagen triple helix stability at pH close to 3.^{22,23} In a general manner, at high ionic strength the formation of salt bridging between triple helices, the presence of low screening (Debye) lengths, or both favor the thermal stabilization of the native collagen conformation.^{22d} At low ionic strength, large screening (Debye) lengths favor the formation of longer-range ion pairs which are mostly destabilizing for the triple helix conformation.^{22d} However, the effect of salt concentration on triple helices stability is not clearly established since, in condition of low salt concentration (concentration below 20 mM), Komsa-Penkova et al.^{22b} has reported that the temperature of collagen denaturation decreases with a factor of about 0.2 °C per 1 mM of NaCl.

In our case, the global salt concentration is determined by the initial NaVO_3 concentration which is equal to the vanadate concentration between 3 mM and 32 mM.

On the one hand, the phase-separation behavior observed at 5 °C reveals that decavanadate species interact with collagen triple helices and can promote triple helix aggregation until the macroscopic phase separation. This is certainly related to a charge matching between negatively charged decavanadate species and positively charged collagen chains. Thus, even if the initial salt concentration is quite low ($[\text{NaVO}_3] \leq 32$ mM), the highly charged decavanadate clusters are apparently able to stabilize collagen triple helices through electrostatic bridging and possibly through collagen triple-helix dehydration²⁴ notably in the case of the macroscopic phase separation.

On the other hand, the collagen triple helices of the liquid part are present in a low ionic strength medium, which is comparable to collagen samples described by Komsa-Penkova et al.^{22b} for which the temperature of denaturation decreases with the global salt concentration (sodium and vanadates ions), in good agreement with the magnitude of collagen triple helix thermal destabilization of about 0.2 °C/mM of NaVO_3 .

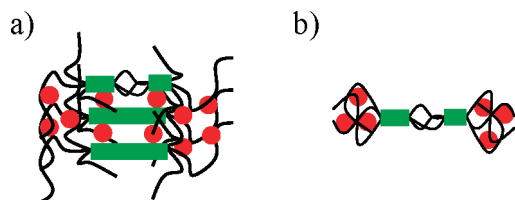
In the context of our initial study concerning vanadate/gelatin mixtures, this set of experiments is in good agreement with the previous measurements performed with partially renatured gelatin (Figure 7). It shows in a clear manner that vanadates interact with native collagen triple helices and can stabilize an important fraction of triple helices against denaturation over a broad range of temperatures (38% of collagen triple helices remain at 47 °C with 32 mM of vanadate) probably via the formation of triple helix aggregates due to vanadate/triple helix bridging.

(d) Discussion and Proposed Mechanism. In order to summarize the different results and to clarify the global picture of the gelatin triple helix renaturation and melting in presence of vanadate, we have represented in Scheme 1 a mechanism that may explain our measurements.

In a first stage, at the beginning of the renaturation process ($T = 50\text{ °C}$), gelatin chains are in a random coil conformation (sketch A.1 in Scheme 1), and vanadate species are homogeneously dispersed in this network (sketch B.1 in Scheme 1).

A certain amount of highly negatively charged decavanadate clusters form physical cross-links between different gelatin chains giving rise to a weak physical gel. The elastic properties of this gel depend exponentially of the vanadate concentration. From $T \approx 40\text{ °C}$, isolated triple helices start to nucleate in systems containing high concentrations of decavanadate (sketch B.2 in Scheme 1). At this point, we can suggest that the presence of vanadate/gelatin cross-links may lead to a decrease of the

SCHEME 2: Schematic Representation of the Two Proposed Mechanisms of Gelatin Triple Helix Stabilization for Temperatures above 40 °C: (a) Formation of Triple Helix Aggregates via Decavanadate Bridging, (b) Formation of Thermally Stable Microgels in the Dangling Ends of Triple Helices^a



^a The red disk represents a decavanadate species; the green rod represents a triple helix; the black solid line represents a gelatin chain.

thermal agitation of the macromolecules and induce locally a better proximity and alignment of gelatin chains, thus promoting the gelatin/gelatin physical interactions. Between 40 and 25 °C, the concentration of isolated triple helices at a given temperature is slightly higher in samples with higher vanadate contents (sketch B.2 in Scheme 1). At the critical triple helix concentration ($C_{hel}^* \approx 0.004 \text{ g} \cdot \text{cm}^{-3}$), an extended triple helix network starts to form. At this stage, the contribution of vanadates to the network elasticity decreases rapidly and becomes non measurable at 20 °C. At this temperature, the helix concentration and G' modulus are almost independent of the vanadate concentration (sketches A.3 and B.3 in Scheme 1). Moreover, the distribution of the vanadate species in the system has probably strongly changed because of the triple helix network formation. According to the convergence of all the G' curves toward the pure gelatin curve of elasticity at 20 °C (Figure 3b) and to the significant influence of the vanadate concentration on the viscous modulus at 20 °C (Figure 2b), one can suggest that the decavanadate are mainly concentrated in the dangling parts of the triple helix network. Therefore, in contrast to the beginning of the renaturation process, the vanadate distribution in the gelatin network is probably anisotropic/inhomogeneous at the mesoscopic length scale.

In a second stage, when the temperature starts to increase, the melting of triple helices probably begins in regions where no or few decavanadates are present (sketch B.4 in Scheme 1). Above 25 °C, the kinetics of triple helices melting seems to be disfavored in presence of vanadates, and in a final stage, above 30 °C, an equilibrium state is reached (sketch B.5 in Scheme 1). According to our measurements, two mechanisms of triple helix stabilization can be proposed: (1) vanadate species promote the formation of stable triple helix aggregates via electrostatic bridging (Scheme 2a), and (2) the presence of vanadates at large concentration in the dangling end of the triple helices may promote the formation of thermally stable vanadate/gelatin microgels (Scheme 2b) as observed in a previous study.¹⁸ The presence of these strong and thermally stable cross-links in the dangling ends of the triple helices may also have a stabilizing effect on triple helices against thermal agitation. This last scenario should additionally explain the modification of the vanadate cross-links distribution in the system as supported by rheology above 35 °C (see Figure 6 and the related description).

IV. Summary and Conclusion

We report the first detailed study concerning the influence of decavanadate clusters on gelatin rheological properties and transition of conformation at pH 3.4, in the semidilute regime of concentration and over a wide range of temperatures. We

have considered gelatin extracted from porcine skin (type A, $M_w \approx 40\,000 \text{ g} \cdot \text{mol}^{-1}$, IEP ≈ 8) and decavanadate clusters ($[\text{H}_2\text{V}_{10}\text{O}_{28}]^{4-}$) that are an interesting model system for POMs of low size.

During triple helix renaturation (50 °C \rightarrow 20 °C), we have shown that, when gelatin chains are in coil conformation (27 °C $< T < 50$ °C), the decavanadate clusters act as physical cross-linkers governing the visco-elastic properties of the mixture ($G' \propto e^{15.4*[\text{vanadate}]}$, $G'' \propto e^{10.2*[\text{vanadate}]}$). This weak physical network slightly favors the gelatin triple helix nucleation. When gelatin chains form an extended triple helices network (20 °C $< T < 27$ °C), the elastic component of the physical gel increases significantly and is governed by the triple helix concentration in good agreement with the gelatin master curve of elasticity recently established by Joly-Duhamel et al.^{10b,c} whereas the viscous counterpart keeps a strong dependence with vanadate concentration ($G'' \propto e^{5.0*[\text{vanadate}]}$) in contrast with chemically cross-linked gelatin. We highlight that the presence of a gelatin/decavanadate weak physical gel since $T = 50$ °C enables the detection of the onset of isolated triple helices formation and percolation via rheological measurements by mean of $\tan \delta$ curves displaying a peak in this region not reported so far.

During the triple helix melting (20 °C \rightarrow 50 °C), we revealed the nonfully reversible behavior of the vanadate/gelatin rheological properties and stabilization of gelatin triple helices due to vanadate species until 50 °C. This nonreversible character has also been observed in the same experimental conditions with collagen/vanadate solutions. This is the first time that such a stabilization of triple helices has been proposed in the case of gelatin hydrogels chemically cross-linked or not.

On the one hand, we proposed to analyze these original results by considering that decavanadate can promote the formation of stable mesoscopic triple helix aggregates via electrostatic bridging. On the other hand, we believe that the formation of an extended triple helix network should induce an inhomogeneous distribution of vanadate cross-linkers which should be mainly concentrated in the dangling ends of the triple helices. This process may promote the formation of thermally stable microgels that may also have a stabilizing effect on triple helices.

Further studies should be performed to confirm this model. In particular, it would be of high interest to get access to the localization of vanadates within the gelatin network during the renaturation/melting processes, for instance, via small-angle neutron scattering (SANS) techniques. In parallel, a more complete evaluation of collagen-based systems, that present a more homogeneous population of triple helices, together with the study of fish gelatins, that exhibit a lower gelation temperature, will certainly provide a better picture of these complex systems.

On a more general level, our results provide a framework to understand the rheological and structural consequences of the POMs addition on the behavior of biopolymers in a semidilute solution. We hope that this work will motivate further studies to systematically explore the complex and original synergy between well-defined POMs and self-assembling natural macromolecules and will contribute to the development of rational approaches for the synthesis of new functional bionanocomposites.

Acknowledgment. The authors thank Mara Coppola and Dr. Nadia Elharfaoui for sharing their experience in rheology and micro-DSC experiments. The authors also acknowledge Dr. Gervaise Mosser for kindly providing the native collagen solution and for fruitful discussions.

Supporting Information Available: Representation of the heat exchanged during renaturation as measured by μ -DSC and

representation of the corresponding helix concentration evolution as measured by polarimetry in the same condition than the μ -DSC measurements for a gelatin solution ($[G] = 10$ wt %, pH = 3.4). Thermograms obtained by μ -DSC during renaturation and denaturation at 0.05 °C \cdot min $^{-1}$ for gelatin solutions ($[G] = 10$ wt %, pH = 3.4) displaying different vanadate concentrations: $[V] = 0$ mM, 18 mM, 36 mM, and 54 mM. Representations of the storage (G') and loss (G'') modulus as a function of vanadate concentration during the cooling ramp and the heating ramp for different temperatures. This material is available free of charge via Internet at <http://pubs.acs.org>.

References and Notes

- (1) (a) Special issue on polysaccharides I., *Adv. Polym. Sci.* **2005**, 186. (b) Special issue on polysaccharides II., *Adv. Polym. Sci.* **2006**, 205. (c) Rinaudo, M. *Prog. Polym. Sci.* **2006**, 31, 603. (d) Liu, X. D.; Yamada, M.; Matsunaga, M.; Nishi, N. *Adv. Polym. Sci.* **2007**, 209, 149.
- (2) Special issue on polyoxometalates. *Chem. Rev.* **1998**, 98.
- (3) (a) Katsoulis, D. E. *Chem. Rev.* **1998**, 98, 359. (b) Guzmán, J.; Saucedo, I.; Navarro, R.; Revilla, J.; Guibal, E. *Langmuir* **2002**, 18, 1567. (c) Michele, D. E.; Thomsen, D.; Louters, L. L. *Biochimie* **1997**, 79, 457.
- (4) Mann, S. *Biomimetic Materials Chemistry*, Mann, S., Eds.; Wiley-VCH: Weinheim, 1997; pp 1–40.
- (5) (a) Falini, G. *Science* **1996**, 271, 67. (b) Belcher, A. M. *Nature* **1996**, 381, 56. (c) Mirkin, C. A. *Nature* **1996**, 382, 607. (d) Alivisatos, A. P. *Nature* **1996**, 382, 609. (e) Whaley, S. R.; English, D. S.; Hu, E. L.; Barbara, P. F.; Belcher, A. M. *Nature* **2000**, 405, 665. (f) Stupp, S. I.; Donners, J. J. M.; Li, L.-S.; Mata, A. *MRS Bull.* **2005**, 30, 864. (g) Sanchez, C.; Arribart, H.; Giraud Guille, M.-M. *Nat. Mater.* **2005**, 4, 277.
- (6) (a) Lutta, S. T.; Dong, H.; Zavalij, P. Y.; Whittingham, M. S. *Mater. Res. Bull.* **2005**, 40, 383. (b) Darder, M.; Ruiz-Hitzky, E. *Curr. Nanosci.* **2006**, 2, 153. (c) Darder, M.; Aranda, P.; Ruiz-Hitzky, E. *Adv. Mater.* **2007**, 19, 1309.
- (7) (a) Livage, J. *Chem. Scr.* **1988**, 28, 9. (b) Rouxel, J. *Chem. Scr.* **1988**, 28, 33. (c) Gopalakrishnan, J. *Chem. Mater.* **1995**, 7, 1265.
- (8) (a) Ruiz-Hitzky, E.; Darder, M.; Aranda, P. *J. Mater. Chem.* **2005**, 15, 3650. (b) Yu, L. T.; Banerjee, I. A.; Matsui, H. *J. Am. Chem. Soc.* **2003**, 125, 14837. (c) Gao, S. Y.; Zhang, H. J.; Wang, X. M.; Deng, R. P.; Sun, D. H.; Zheng, G. L. *J. Phys. Chem. B* **2006**, 110, 15847. (d) Bauermann, L. P.; del Campo, A.; Bill, J.; Aldinger, F. *Chem. Mater.* **2006**, 18, 2016.
- (9) (a) *The Science and Technology of Gelatin*; Ward, A. G., Courts, A., Eds.; Academic Press: London, 1977. (b) Djabourov, M. *Contemp. Phys.* **1988**, 29, 273–297. (c) Ross-Murphy, S. B. *Polymer* **1992**, 33, 2622. (d) Michon, C.; Cuvelier, G.; Launay, B. *Rheol. Acta* **1993**, 32, 94.
- (10) (a) Sobral, P. J. A.; Habitante, A.M.Q.B. *Food Hydrocolloids* **2001**, 15, 377. (b) Joly-Duhamel, C.; Hellio, D.; Ajdari, A.; Djabourov, M. *Langmuir* **2002**, 18, 7158. (c) Joly-Duhamel, C.; Hellio, D.; Djabourov, M. *Langmuir* **2002**, 18, 7208. (d) Guo, L.; Colby, R. H.; Lusignan, C. P.; Whitesides, T. H. *Macromolecules* **2003**, 36, 9999. (e) Guo, L.; Colby, R. H.; Lusignan, C. P.; Whitesides, T. H. *Macromolecules* **2003**, 36, 10009. (f) Elharfaoui, N.; Djabourov, M.; Babel, W. *Macromol. Symp.* **2007**, 256, 149.
- (11) (a) Schacht, E.; Bogdanov, B.; VandenBulcke, A.; DeRooze, N. *React. Funct. Polym.* **1997**, 33, 109. (b) Kuijpers, A. J.; Engbers, G. H. M.; Feijen, J.; De Smedt, S. C.; Meyvis, T. K. L.; Demeester, J.; Krijgsveld, J.; Zaat, S. A. J.; Dankert, J. *Macromolecules* **1999**, 32, 3325. (c) Hellio-Serughetti, D.; Djabourov, M. *Langmuir* **2006**, 22, 8509. (d) Hellio-Serughetti, D.; Djabourov, M. *Langmuir* **2006**, 22, 8516.
- (12) (a) Chun, S.-W.; Kim, J.-D. *J. Controlled Release* **1996**, 38, 39. (b) Dhara, D.; Rathna, G. V. N.; Chatterji, P. R. *Langmuir* **2000**, 16, 2424. (c) Boudet, C.; Iliopoulos, I.; Poncelet, O.; Cloitre, M. *Biomacromolecules* **2005**, 6, 3073.
- (13) (a) Bowman, W. A.; Rubinstein, M.; Tan, J. S. *Macromolecules* **1997**, 30, 3262. (b) Gillmor, J. R.; Connelly, R. W.; Colby, R. H.; Tan, J. S. *J. Polym. Sci.: Part B* **1999**, 37, 2287. (c) Gilsenan, P. M.; Richardson, R. K.; Morris, E. R. *Food Hydrocolloids* **2003**, 17, 723.
- (14) (a) Greener, J.; Constestable, B. A.; Bale, M. D. *Macromolecules* **1987**, 20, 2490. (b) Whitesides, T. H.; Miller, D. D. *Langmuir* **1994**, 10, 2899. (c) Griffiths, P. C.; Stilbs, P.; Howe, A. M.; Whitesides, T. H. *Langmuir* **1996**, 12, 5302.
- (15) (a) Bloomfield, V. A. *Curr. Opin. Struct. Biol.* **1996**, 6, 334. (b) He, S.; Arscott, P. G.; Bloomfield, V. A. *Biopolymers* **2000**, 53, 329. (c) Yamada, M.; Yokota, M.; Kaya, M.; Satoh, S.; Jonganurakkun, B.; Nomizu, M.; Nishi, N. *Polymer* **2005**, 46, 10102.
- (16) (a) Pope, H. T. *Heteropoly and Isopoly Oxometalates*; Springer-Verlag: New York, 1983. (b) Livage, J. *Chem. Mater.* **1991**, 3, 578. (c) Livage, J. *Coord. Chem. Rev.* **1998**, 178–180, 999.
- (17) (a) Evangelou, A. M. *Crit. Rev. Oncol./Hematol.* **2002**, 42, 249. (b) Crans, D. C.; Smee, J. J.; Gaidamauskas, E.; Yang, L. *Chem. Rev.* **2004**, 104, 849. (c) Ashraf, S. M.; Kaleem, S. *Anal. Biochem.* **1995**, 230, 68.
- (18) Carn, F.; Steunou, N.; Djabourov, M.; Coradin, T.; Ribot, F.; Livage, J. *Soft Matter* **2008**, 4, 735.
- (19) (a) Turgeon, S. L.; Schmitt, C.; Sanchez, C. *Curr. Opin. Colloid Interface Sci.* **2007**, 12, 166. (b) Griffiths, P. C.; Stilbs, P.; Howe, A. M.; Cosgrove, T. *Langmuir* **1996**, 12, 2884. (c) Griffiths, P. C.; Stilbs, P.; Howe, A. M.; Whitesides, T. H. *Langmuir* **1996**, 12, 5302. (d) Griffiths, P. C.; Abbott, R.; Stilbs, P.; Howe, A. M. *Chem. Commun.* **1998**, 53. (e) Thunemann, A. F.; Muller, M.; Dautzenberg, H.; Joanny, J. F.; Lowen, H. *Adv. Polym. Sci.* **2004**, 166, 113. (f) Zhang, H.; Dubin, P. L.; Ray, J.; Manning, G. S.; Moorefield, C. N.; Newkome, G. R. *J. Phys. Chem. B* **1999**, 103, 2347.
- (20) Giraud-Guille, M.-M.; Besseau, L.; Herbage, D.; Gounon, P. *J. Struct. Biol.* **1994**, 113, 99.
- (21) Harrington, W. F.; Rao, N. V. *Conformation of Biopolymers*; Academic Press: New York, 1967; Vol. 2.
- (22) (a) Bianchi, E.; Conio, G. *J. Biol. Chem.* **1967**, 242, 1361. (b) Komsa-Penkova, R.; Koynova, R.; Kostov, G.; Tenchov, B. G. *Biochim. Biophys. Acta* **1996**, 1297, 171. (c) Brown, E. M.; Farrell, H. M.; Wildermuth, R. J. *J. Protein Chem.* **2000**, 19, 85. (d) Freudenberg, U.; Behrens, S. H.; Welzel, P. B.; Muller, M.; Grimmer, M.; Salchert, K.; Taeger, T.; Schmidt, K.; Pompe, W.; Werne, C. *Biophys. J.* **2007**, 92, 2108.
- (23) Ibarra-Molero, B.; Zitzewitz, J. A.; Matthews, C. R. *J. Mol. Biol.* **2004**, 336, 989.
- (24) Miles, C. A.; Avery, N. C.; Rodin, V. V.; Bailey, A. J. *J. Mol. Biol.* **2005**, 346, 551.